

experiment, especially considering the lack of adjustable parameters. It is particularly noteworthy that this calculation reproduces the mild temperature dependence in the methanol solution, where the deviations from simple hydrodynamic behavior are the greatest.

The Enskog model considers uncorrelated binary collisions and does not take into account the correlated collective motions that contribute to the macroscopic viscosity. Thus, the agreement of the Enskog model with the experimental torsional correlation times suggests that short-range molecular interactions are the important factor in determining the well friction in gauche *n*-butane and that the torsional fluctuations are weakly coupled to the collective viscous modes of the solvent. We do not believe this weak coupling results from the frequency dependence of the friction, since the well friction probed in our half-width measurements is a zero-frequency (or at least low-frequency) friction. Instead, it may be that the small amplitude of the torsional fluctuations emphasizes the short distance, or high wavevector friction, which is determined primarily by binary, uncorrelated events.^{100,101} A similar argument has been put forth by Oxtoby in order to explain the success of the binary collision model in describing vibrational relaxation data.¹⁰² This view may also be related to the concept of "inner and outer solvent zones" around a solute.^{44,89}

Conclusions

Our measurements show the variation in ΔH to be relatively small for all of the solvents studied here, as well as for those studied previously. The values of ΔH in the different solvents do not

correlate in any simple fashion with macroscopic solvent parameters. The experimental torsional correlation times and well friction show dramatic deviations from the simple linear dependence on viscosity predicted by hydrodynamic models of solvent friction, with the deviations being most pronounced for methanol. Similar, but less dramatic, deviations are observed for the rotational correlation times. The dependence of the torsional correlation times on viscosity is well represented by a power law for all solvents. Alternatively, excellent agreement with experiment is obtained by using an Enskog collisional model for friction. The success of the Enskog model may indicate that the well friction is determined by the short distance or high wavevector solvent friction.

We have presented a comprehensive experimental study of well friction for a simple isomerization reaction in solution. An understanding of this well friction is crucial to the understanding of isomerization rates in the low-friction, energy-controlled regime, and possibly in the very high friction regime as well.¹⁰³⁻¹⁰⁵ We hope our results will stimulate further theoretical work and computer simulations on *n*-butane dynamics in solution and that such work will lead to a clearer picture of solvent friction in liquid-state reactions.

Acknowledgment. We gratefully acknowledge the National Science Foundation (CHE-8607230) for partial support of this research. We also thank the reviewers for helpful, constructive comments and for drawing ref 52 to our attention.

(100) Oxtoby, D. W. *Mol. Phys.* **1977**, *34*, 987.

(101) Alley, W. E.; Alder, B. J.; Yip, S. *Phys. Rev. A* **1983**, *27*, 3174.

(102) Oxtoby, D. W. *J. Chem. Phys.* **1979**, *70*, 2605.

(103) Straub, J. E.; Borkovec, M.; Berne, B. J. *J. Chem. Phys.* **1986**, *84*, 1788.

(104) Okuyama, S.; Oxtoby, D. W. *J. Chem. Phys.* **1986**, *84*, 5830.

(105) Barrat, J.-L. *Chem. Phys. Lett.* **1990**, *165*, 551.

Electric Field Effects on Emission Line Shapes When Electron Transfer Competes with Emission: An Example from Photosynthetic Reaction Centers

David J. Lockhart, Sharon L. Hammes, Stefan Franzen, and Steven G. Boxer*

Department of Chemistry, Stanford University, Stanford, California 94305 (Received: June 13, 1990)

Electron-transfer reactions are expected to be particularly sensitive to externally applied electric fields because of the presence of charge-separated, dipolar states, and the effects of the field on photoinduced reactions can be determined by monitoring the competing emission. The rates of photoinduced electron-transfer reactions between a donor and acceptor are often measured by comparing the quantum yield of the competing emission from the state undergoing the reaction in the presence and absence of electron transfer. Calculations are presented for the fluorescence line shape and amplitude changes expected for isotropic and oriented samples of molecules undergoing electron transfer in an applied electric field. The calculations are based on a model that includes the expected effects of the field on both the fluorescence transition energy and the rate of the competing electron-transfer reaction. These model calculations indicate that a surprisingly wide range of electric-field-modulated line shapes are possible and that the line shape is very sensitive to key parameters that characterize the electron-transfer reaction. An example of these effects has been obtained in a structurally characterized donor/acceptor system, the bacterial photosynthetic reaction center, whose electric-field-modulated fluorescence changes have been characterized in detail. Information on the magnitude and direction of the dipole moment of the emitting state and on the mechanism and rate versus free energy curve for this picosecond long-distance electron-transfer reaction are obtained by comparing the experimental data with the results of the model calculations.

The rate of photoinduced electron-transfer reactions between a donor and acceptor can be measured by comparing the quantum yield of the competing fluorescence or phosphorescence from the state undergoing the reaction in the presence and absence of electron transfer. Usually the integrated amplitude of the emission and the intensity at any emission wavelength can be used interchangeably because the emission-quenching reaction changes only the amount of emission and not its line shape. In an earlier paper

we demonstrated that if the rate of the electron-transfer reaction that competes with emission depends on the molecular orientation relative to some axis, such as that defined by an externally applied electric field, then the field effects on the competing reaction cause the fluorescence from an isotropic sample to become polarized.¹ In the present paper we demonstrate that these effects can also lead to a change in the emission line shape. This extension and generalization was motivated by earlier studies of the effects of

* Address correspondence to this author.

(1) Lockhart, D. J.; Boxer, S. G. *Chem. Phys. Lett.* **1988**, *144*, 243.

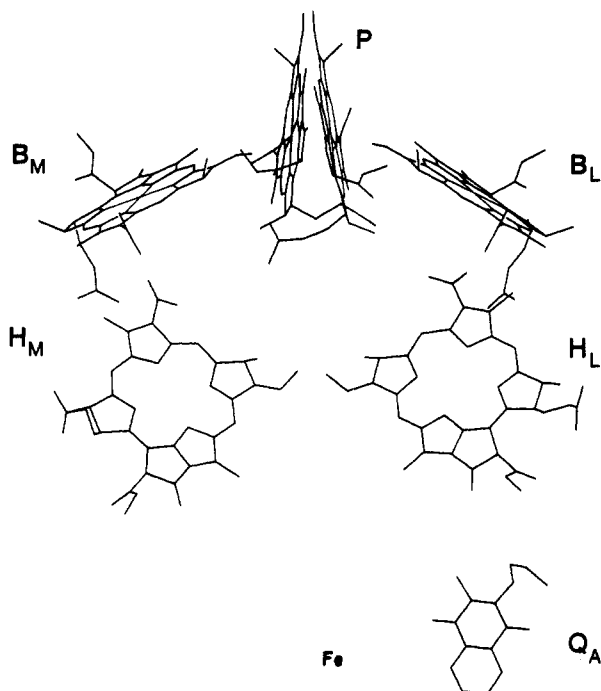


Figure 1. Arrangement of the chromophores participating in the initial electron-transfer reactions, taken from the X-ray coordinates for *Rps. viridis* RCs.²¹⁻²³ A nearly identical figure is obtained for *Rb. sphaeroides*.³⁸⁻⁴⁰ The direction of the transition dipole moments for the fluorescence and the Q_y transition of P is approximately perpendicular to the page passing through the point at the geometric center of P. An approximate C_2 symmetry axis is directed along a line that runs from the geometric center of P to the non-heme iron atom.

electric fields on the fluorescence from bacterial photosynthetic reaction centers.^{1,2} In the following we discuss these results in detail, develop a general model for the induced line-shape changes, including some examples of the surprisingly large range of effects that might be observed under specific realizable circumstances, and conclude with a detailed analysis of the data for reaction centers.

The fluorescence quantum yield for immobilized, isotropic samples of photosynthetic reaction centers (RCs) increases upon application of an electric field at cryogenic temperatures.^{1,2} We have proposed a physical mechanism to explain this result that involves a net slowing of the rate of the initial electron-transfer step which competes with fluorescence.^{1,2} This interpretation has been confirmed by direct measurements of the electric field dependence of the kinetics.^{3,4} The absolute magnitude, field dependence, and line shape of the field effect on the fluorescence were not previously considered in detail. In this paper we focus on these factors using a physical model that contains the *minimum* number of structural and energetic parameters that must be used in *any* treatment of electric-field effects on electron-transfer reaction dynamics, whether in the RC or in other systems. The model calculations demonstrate that the specific experimental results for the RC constrain the values of these parameters to a rather narrow range with significant consequences for understanding the mechanism of charge separation.

Charge separation in photosynthetic reaction centers is initiated by electronic excitation of a dimer of bacteriochlorophyll molecules, known as the special pair or P (Figure 1). The nature of the initially formed singlet excited state of P (1P) and its time evolution have been the subject of a great deal of interest and investigation. We approached this problem, as did others, by

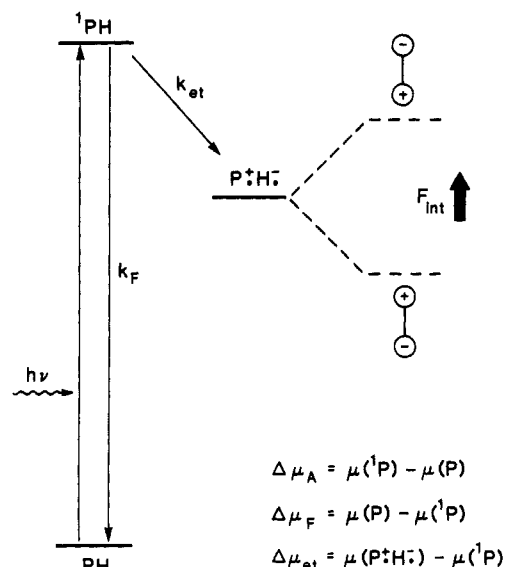


Figure 2. Reaction scheme describing the initial events in bacterial photosynthetic RCs (cf. Figure 1). In the absence of a subpicosecond decay of the initially formed excited state, the emitting state is 1P . The definitions given for the difference dipoles in the figure assume that 1P is the emitting state (see text). The solid lines are schematic energy levels at zero field. For an isotropic, immobilized sample in an electric field, the energy of any dipolar state increases or decreases depending on the orientation of the permanent electric dipole of the state relative to the field. The largest changes occur for dipoles oriented parallel or antiparallel to the field, as illustrated with dashed lines for the P^+H^- state.

measuring the effect of an electric field on the absorption line shape (the Stark effect) of the lowest energy electronic Q_y transition of P.⁵⁻¹¹ It was found that in an immobilized, isotropic sample of RCs the Q_y band of P becomes broader in the presence of the field (the change in absorption, ΔA , spectrum has a primarily second derivative line shape), as expected if there is a permanent electric dipole moment difference, $\Delta\mu_A$, between the ground and excited states [$\Delta\mu_A = \mu(^1P) - \mu(P)$] (see Figure 2). Assuming that the ground state of P is relatively nonpolar, the results of this experiment indicate that the state 1P is considerably more dipolar than the lowest energy singlet excited state of a monomeric bacteriochlorophyll, possibly due to mixing with charge-transfer states.^{12,49-51}

To determine if the state 1P subsequently evolves on a subpicosecond time scale, as has been suggested by some investigators,^{13,14} we measured the effect of an electric field on the prompt fluorescence from RCs. The dipole moment difference between the emitting and ground state, $\Delta\mu_F$, by comparison with $\Delta\mu_A$, allows the determination of whether the state formed upon direct electronic excitation of P is the same as the one that emits for several picoseconds following excitation. To our surprise, the

(5) DeLeeuw, D.; Malley, M.; Buttermann, G.; Okamura, M. Y.; Feher, G. *Biophys. Soc. Abstr.* **1982**, *37*, 111a.

(6) Lockhart, D. J.; Boxer, S. G. *Biochemistry* **1987**, *26*, 664-668; *Ibid.* **1987**, *26*, 2958.

(7) Boxer, S. G.; Lockhart, D. J.; Middendorf, T. R. *Springer Proc. Phys.* **1987**, *20*, 80-90.

(8) Lockhart, D. J.; Boxer, S. G. *Proc. Natl. Acad. Sci. U.S.A.* **1988**, *85*, 107-111.

(9) Lösche, M.; Feher, G.; Okamura, M. Y. *Proc. Natl. Acad. Sci. U.S.A.* **1987**, *84*, 7537.

(10) Lösche, M.; Feher, G.; Okamura, M. Y. In *The Photosynthetic Bacterial Reaction Center—Structure and Dynamics*; Breton, J., Vermeglio, A., Eds.; Plenum: New York, 1988; pp 151-164.

(11) Braun, H. P.; Michel-Beyerle, M. E.; Breton, J.; Buchanan, S.; Michel, H. *FEBS Lett.* **1987**, *221*, 221-225.

(12) Boxer, S. G.; Goldstein, R. A.; Lockhart, D. J.; Middendorf, T. M.; Takiff, L. T. *J. Phys. Chem.* **1989**, *93*, 8280-8294.

(13) Meech, S. R.; Hoff, A. J.; Wiersma, D. A. *Chem. Phys. Lett.* **1985**, *121*, 287-292.

(14) Meech, S. R.; Hoff, A. J.; Wiersma, D. A. *Proc. Natl. Acad. Sci. U.S.A.* **1986**, *83*, 9464-9468.

(2) Lockhart, D. J.; Goldstein, R. F.; Boxer, S. G. *J. Chem. Phys.* **1988**, *88*, 1408-1415.

(3) Boxer, S. G.; Lockhart, D. J.; Kirmaier, C.; Holten, D. In *Perspectives in Photosynthesis*; Jortner, J., Pullman, B., Eds.; Elsevier: Amsterdam, 1989; Kluwer: Boston, 1990; pp 39-52.

(4) Lockhart, D. J.; Kirmaier, C.; Holten, D.; Boxer, S. G. *J. Phys. Chem.* **1990**, *94*, 6987.

dominant effect of an electric field on the fluorescence from RCs at 77 K is to increase the quantum yield^{1,2} with very little, if any, contribution due to a line broadening. Within the model of an isotropic distribution of emitting molecules, this was interpreted to indicate that $|\Delta\mu_F| \leq |\Delta\mu_A|$; in fact, the data were found to be consistent with $|\Delta\mu_F| = 0$ D, which seems physically unlikely. It was also found that the ΔF (change in fluorescence) spectrum is somewhat red shifted relative to the fluorescence spectrum. The apparent absence of a line broadening (second derivative shaped) contribution to the ΔF spectrum and the presence of the red shift were not readily accounted for with the simple model used in the original paper.² The present paper describes a more complete and realistic model that includes the effects of orientation-dependent competition between fluorescence and electron transfer in an electric field. This model readily accounts for both the apparent absence of a second derivative contribution and the presence of the red shift of the ΔF spectrum and also provides additional information about the early reaction dynamics in bacterial RCs. The model presented should be generally applicable for the study of both emitting states and any field-dependent reactions that compete with emission.

Because the dominant effect of the electric field on the fluorescence was not found to be on the line shape but on the fluorescence intensity, we consider the origin of the fluorescence quantum yield. The quantum yield of fluorescence, Φ_F , is determined by the relative magnitudes of the rates of radiative and nonradiative processes from the emitting state:

$$\Phi_F = k_F / (k_F + k_{nr} + k_{et}) \quad (1)$$

where k_F is the radiative rate, k_{et} is the rate of a competing electron-transfer reaction, and k_{nr} is the combined rate of all other nonradiative processes. If any of these rates is electric-field dependent, then Φ_F is also, resulting in a change in the fluorescence quantum yield that is observable as a change in the *amplitude* of the fluorescence band. k_F and k_{nr} are assumed to be field independent, as is determined to be the case for bacteriochlorophyll *a* and bacteriopheophytin *a* by the absence of a significant change in the net fluorescence intensity for these molecules in an applied electric field at 77 K.² Furthermore, there is very little change, if any, in the oscillator strength for the Q_y absorption transition of P as determined by the line shape of the absorption Stark effect spectrum.^{6,8-10} If the emitting state is the same as that formed upon absorption into the Q_y band of P, then k_F , which is proportional to the oscillator strength, is relatively field independent. k_{et} , on the other hand, is expected to be sensitive to an electric field for an electron-transfer reaction between neutral molecules because such a reaction produces a charge-separated, dipolar state whose energy will be strongly dependent on field. The exact dependence of k_{et} on an applied electric field is determined largely by its dependence on the free energy difference between the electron-transfer final and initial states,¹⁵ which, in turn, depends on the permanent electric dipole moment difference between these states, $\Delta\mu_{et} = \mu(P^{*+}I^{-}) - \mu(^1P)$, where I is the initial electron acceptor. Thus, an externally applied electric field is expected to have an effect on both the fluorescence line shape and the fluorescence amplitude. The analysis of the effect of an electric field on the fluorescence spectrum therefore allows one to obtain information on both the initial and final states of an electron-transfer reaction by determining $\Delta\mu_F$ and $\Delta\mu_{et}$, respectively.

The nonradiative rate constant k_{nr} may also be sensitive to an external electric field. The electric-field dependence of the nonradiative rate is likely to be considerably weaker than that of the electron-transfer rate because the difference dipole moment for the nonradiative step between the emitting and ground state is much smaller than the difference dipole for electron transfer. In the case of the RC, the difference dipole moment between the state 1P and the ground-state P is sufficiently large that the electric-field effect on k_{nr} may play a role in the field dependence of the emission. We shall ignore possible field effects on k_{nr} in the following analysis based on the bacteriochlorophyll *a* results

and on the above reasoning and because no data are yet available on the effects of an electric field on the properties of an RC that lacks the electron acceptor. Electric-field-effect experiments on the emission of a model porphyrin dimer suggest that any electric-field effects on the nonradiative rate are small compared to the effect on the line shape due to electron transfer (Lockhart, D. J., unpublished results).

In the original papers on the electric-field-induced emission anisotropy in the RC, the effects due to $\Delta\mu_F$ and $\Delta\mu_{et}$ were treated independently, i.e., $\Delta\mu_F$ was determined by analyzing the line-broadening (second derivative) contribution to the ΔF spectrum, and the amplitude change (zeroth derivative contribution to the ΔF spectrum) was analyzed in terms of $\Delta\mu_{et}$.^{1,2} Although a reasonable start, there is a potential shortcoming in this approach. A permanent electric dipole moment difference between the ground and excited state results in a pure line broadening of the absorption or emission spectrum in the presence of an electric field only in the case of a perfectly isotropic distribution of absorbing or emitting molecules. This condition is easily satisfied in an absorption electric-field effect experiment by preparing the sample in a way that leads to no orientational preference (e.g., a poured polymer film or a frozen glass). In a fluorescence experiment an orientationally isotropic sample as well as isotropic excitation of the emitting molecules is required. This is also easily achieved by using unpolarized excitation light at appropriate wavelengths. However, anisotropy in the distribution of emitting molecules can be *dynamically* produced by virtue of competing electric-field-dependent electron transfer. Anisotropy is produced because k_{et} is expected to depend on the relative directions of the applied field and $\Delta\mu_{et}$, so that the probability of fluorescence from any particular molecule (or any particular orientational subpopulation) following excitation is orientation dependent. The shift in energy levels that gives rise to an orientation dependent rate is depicted in Figure 2. The fluorescence quantum yield is therefore orientation dependent, causing the emission from an isotropically prepared distribution of emitting molecules to become anisotropic or polarized. This effect has been observed by us on the fluorescence from RCs¹ and was used to study the mechanism of the initial electron-transfer reaction. This electric-field-induced fluorescence anisotropy therefore complicates the analysis of $\Delta\mu_F$ because a simple analysis assuming an isotropic distribution of emitting molecules is not entirely valid. To determine $\Delta\mu_F$ quantitatively, it is necessary to know the form of the weighted (anisotropic) distribution, with the weighting factor (probability of emission) in an electric field determined by k_{et} through its dependence on $\Delta\mu_{et}$. As will be shown in the following, an analysis of this complication (when combined with other independently obtained data for the RC) introduces the opportunity to determine not only the magnitude of $\Delta\mu_F$ but also the relative directions of $\Delta\mu_F$ and $\Delta\mu_{et}$ and the dependence of k_{et} on the applied field perturbation.

Theory

The Model. The basic kinetic scheme upon which the model is based is shown in Figure 2. The effects described in this paper are a direct consequence of this simple scheme and do not require the inclusion of any additional physical mechanism. Many of the angular and dipolar factors are illustrated in Figure 4. The fluorescence quantum yield is given by eq 1. Because k_{et} is large for the reaction being considered in the RC, we assume that k_F and k_{nr} are small relative to k_{et} (quantitatively consistent with the low fluorescence quantum yield, measured to be about 4×10^{-4} at room temperature¹⁶) and that k_{et} is the only field-dependent rate. In this case

$$\Phi_F \propto 1/k_{et} \quad (2)$$

The extent of the field-induced emission anisotropy is determined by the dependence of Φ_F (or k_{et}) on the electric-field perturbation, assumed to be primarily determined by $\Delta\mu_{et} \cdot F_{int}$, where F_{int} is the

(15) Marcus, R. A.; Sutin, N. *Biochim. Biophys. Acta* **1985**, *811*, 265-322.

(16) Zankel, K. L.; Reed, D. W.; Clayton, R. K. *Proc. Natl. Acad. Sci. U.S.A.* **1968**, *61*, 1243.

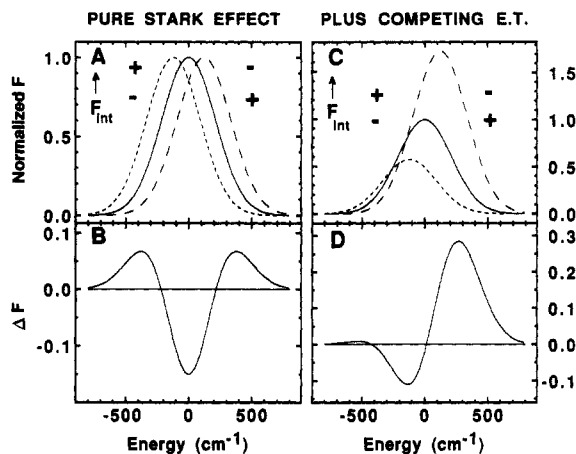


Figure 3. Schematic diagram illustrating the combined consequences of an electric-field-induced band shift and an orientation-dependent competing process. The parameters used to generate the figure are related to those in the RC problem. For the purpose of illustration the hypothetical sample consists of two populations. One population has the C_2 axis of the RC aligned with the externally applied field (---) such that the charge-transfer dipoles make an angle θ with the field, while the other population has the C_2 axis opposing the externally applied field (--) and the charge-transfer dipole, $\Delta\mu_{et}$, makes an angle $\pi - \theta$ with the field. (A) The Gaussian fluorescence line shape for an oriented sample at zero field (solid line) as well as the fluorescence from the two populations when no competing process is present. (B) The ΔF spectrum (field-on minus field-off) of the oriented sample with band shifts shown in panel A. The ΔF spectrum is closely approximated by the second derivative of the zero-field line shape. The parameters used are $\theta = 48^\circ$, $\Delta\mu_F = 10$ D, $\Delta\mu_{et} = 80$ D, $\gamma = 27^\circ$, $\zeta_F = 38^\circ$, and $\zeta_{et} = 65^\circ$. In addition, $P_i = 0$ for all i and $F_{int} = 10^6$ V/cm. (C) The Gaussian fluorescence line shape for an oriented sample at zero field (solid) as well as for the two orientations in an electric field when there is a competing process that is also field dependent. The molecules with the projection of the charge-transfer dipole aligned with the applied field (---) have a diminished fluorescence quantum yield, while those opposed to the field direction (--) have an enhanced fluorescence quantum yield. All parameters are identical with those in panel A except that $P_1 = 6.0 \times 10^{-4}$. (D) The ΔF spectrum of the oriented sample with band shifts shown in panel C. The resulting blue shift is a result of the relative direction of the projections of $\Delta\mu_{et}$ and $\Delta\mu_F$ as well as the sign of P_1 (see text).

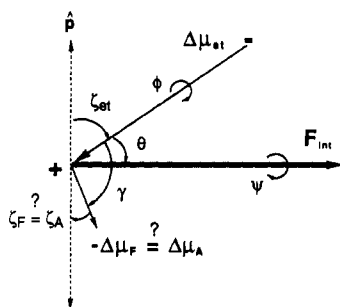


Figure 4. Parameters relevant to the electric field modulation of fluorescence are shown along with the angles for orientation averaging ϕ , θ , and ψ . The angle ψ is the azimuthal angle in the lab frame. F_{int} has the same direction as the externally applied field F_{ext} provided the local field correction factor f is a scalar. The angle ϕ is the azimuthal angle in the molecular frame, and θ is the angle between the Z axis in the lab frame (given by F_{int}) and the z axis in the molecular frame that lies along $\Delta\mu_{et}$. The other angles are fixed in the molecular frame: γ is the angle between $\Delta\mu_{et}$ and $-\Delta\mu_F$, ζ_{et} is the angle between $\Delta\mu_{et}$ and the transition dipole moment p , and ζ_F is the angle between $\Delta\mu_F$ and p (the absorption and fluorescence transition moments are taken as parallel to simplify the figure). Note that the directions of dipole moments follow standard conventions.

electric field actually experienced by the reactive system due to the applied voltage. F_{int} is related to the externally applied electric field F_{ext} (given by the applied voltage divided by the distance between the electrodes), by the equation $F_{int} = fF_{ext}$. The local field correction f is determined by the dielectric properties of the environment; its value is uncertain but is constrained by most

treatments to be in the range between about 1.2 and 1.8.^{6,9,10,17,18} In this case the change in the electric field experienced by the reacting system due to the applied voltage is *larger* than the externally applied field as given by the applied voltage divided by the separation between the electrodes.

The electric-field dependence of Φ_F is modeled as a cumulant expansion in powers of the field perturbation:

$$\Phi_F(F_{int}) = \exp\left(\sum_i P_i (-\Delta\mu_{et} \cdot F_{int})^i\right) \quad (3)$$

A cumulant expansion was used to describe the dependence of Φ_F on the field because it is a general and versatile function⁴⁴ that eliminates any bias or preconceptions about the form of Φ_F or k_{et} , while also ensuring that $\Phi_F(F_{int})$ is positive for all values of $\Delta\mu_{et}$ and F_{int} . For the specific case of field-modulated fluorescence from *Rb. sphaeroides* RCs, this expansion is truncated after three terms because three terms are sufficient to simulate the experimental observables (vide infra). The coefficients of this expansion are determined through the following analysis and have physical meaning with respect to the rate versus electric field curve: $-P_1$ describes the slope, $-P_2$ describes the curvature, and $-P_3$ describes the skewness of the curve about the zero-field value of k_{et} . This allows direct comparison with kinetic studies such as those of Franzen et al.¹⁹ The cumulants obtained from the data analysis can be directly related to a moment expansion of the quantum mechanical expression for the electron-transfer rate.⁴⁴ The moment expansion of the k_{et} vs ΔG_{et} curve is closely related to the well-known moment expansion of line shapes.^{45,46}

We assume that the excitation conditions (unpolarized light at 532 nm or unpolarized broadband light between 350 and 600 nm) produce an initially isotropic distribution of the excited molecules, consistent with the results of linear dichroism measurements.²⁰ For the purpose of the model calculations and without attempting to quantitatively fit the fluorescence line shape, the fluorescence line shape is treated as a sum of the line shapes of the emission from the individual orientational subpopulations, each one approximated by a Gaussian centered at ν_0 with full width at half-maximum (fwhm) equal to 500 cm^{-1} at zero applied field. In the presence of the field, the fwhm of each individual Gaussian is unchanged but the band centers shift to $\nu_0 + \Delta\mu_F \cdot F_{int}$, and $\Delta\mu_F$ is assumed to be the same for all populations (as in the analysis of the usual absorption or emission Stark effect²¹). The normalized fluorescence line-shape function is

$$S(\nu, F_{int}) = \exp\{-4 \ln 2 ([\nu - (\nu_0 + \Delta\mu_F \cdot F_{int})] / \text{fwhm})^2\} \quad (4)$$

The choice of a Gaussian line shape is motivated by the observed shape of the fluorescence spectrum of P in bacterial RCs, which is nearly Gaussian. It is assumed that the line-shape function itself is independent of the electric field. This same assumption is made in the analysis of the absorption Stark effect of P⁵⁻¹⁰ and in the theory of electrochromism in general.^{47,48} The method described in this paper can be applied using an arbitrary line shape and is not dependent on the Gaussian form used in eq 4. The results obtained by using the Gaussian model are nearly identical with those obtained with numerical procedures that use the experimental fluorescence spectrum as the line-shape function (not shown).

The relative contribution to the total emission spectrum from any orientational subpopulation is determined by the field-independent value of the cosine squared of the angle between the direction of the emission transition dipole moment and the polarization direction of the polarizer through which the fluorescence

(17) Chen, F. P.; Hanson, D. M.; Fox, D. *J. Chem. Phys.* **1975**, *63*, 3878-3885.

(18) Böttcher, C. J. F. *Theory of Electric Polarization*; Elsevier: New York, 1973; pp 159-204.

(19) Franzen, S.; Goldstein, R. F.; Boxer, S. G., *J. Phys. Chem.* **1990**, *94*, 5135-5149.

(20) Rafferty, C. N.; Clayton, R. K. *Biochim. Biophys. Acta* **1979**, *545*, 106-121.

(21) Mathies, R. A. Ph.D. Dissertation, Cornell University, 1974.

is collected (the usual photoselection effect) and by the field-dependent value of Φ_F , which depends on $\Delta\mu_{et}\cdot F_{int}$. Specifically, the fluorescence spectrum as a function of ν in the presence of an electric field is calculated by using eq 5,

$$F(\nu, F_{int}) \propto \int \int \int (\mathbf{e}\cdot\mathbf{p})^2 \Phi_F(F_{int}) S(\nu, F_{int}) \sin \theta \, d\theta \, d\phi \, d\psi \quad (5)$$

where \mathbf{e} is a unit vector in the direction of the polarization of the analyzing polarizer, \mathbf{p} is a unit vector in the direction of the fluorescence transition dipole moment, $\Phi_F(F_{int})$ is as given in eq 3, $S(\nu, F_{int})$ is the normalized fluorescence line-shape function, and θ , ϕ , and ψ are the Euler angles. For an initially isotropically prepared distribution of emitting molecules, the integration is over the range $0 \leq \theta \leq \pi$, $0 \leq \phi \leq 2\pi$, $0 \leq \psi \leq 2\pi$. For an oriented sample, when $\Delta\mu_{et}$ makes an angle θ with the field F_{int} (see Figure 4), integration over the angle ψ suffices to calculate $\Phi_F(F_{int})$.

Parameters in the Model. The parameters included in the model are listed below. Many of these parameters are constrained to be in a very narrow range or ranges of values either because of the physical constraints imposed by the structure of the system being considered or because their values can be independently determined by other experiments.

(1) $\Delta\mu_{et}$ is the vector difference between the permanent electric dipole moments of the initial and final states of the electron-transfer reaction. Since the final state of the electron-transfer reaction is much more dipolar than the initial state, *vide infra*, $\Delta\mu_{et}$ is determined primarily by the electron-transfer product state. Using the *Rps. viridis* crystal structure coordinates²²⁻²⁴ and assuming that for the purpose of calculating dipoles the charge distributions in the anion and cation radicals can be approximated by point charges at the center of the respective macrocycles, the magnitudes of $\mu(P^{*+}H_L^{-})$ and $\mu(P^{*+}B_L^{-})$ are estimated to be about 80 and 50 D, respectively.⁵²

(2) $\Delta\mu_F$ is the vector difference between the ground and emitting state permanent electric dipole moments. Assuming that the ground state is relatively nonpolar, $\Delta\mu_F$ is a measure of the emitting state permanent electric dipole moment. It is evident from eqs 4 and 5 that if $\Delta\mu_F = 0$ D, there can be no shift in the maximum of the ΔF spectrum because the shift in the fluorescence spectrum for each orientational subpopulation is determined by the factor $S(\nu, F_{int})$. In the absence of a subpicosecond decay of 1P , 1P is the emitting state and $\Delta\mu_F = \mu(P) - \mu(^1P) \sim -\mu(^1P)$. The magnitude and direction of $\Delta\mu_F$ are to be determined. The magnitude of $\Delta\mu_A = \mu(^1P) - \mu(P)$ has been determined to be about 7 D/f at 77 K.^{8,9} ζ_A is the angle between $\Delta\mu_A$ and the transition dipole moment of the Q_y transition of P, which has been determined by absorption Stark effect measurements to be $38 \pm 2^\circ$ at 77 K.^{8,9}

(3) ζ_{et} is the angle between the emission transition dipole moment and $\Delta\mu_{et}$. This angle is to be determined.

(4) ζ_F is the angle between the emission transition dipole moment and $\Delta\mu_F$; its value is to be determined. ζ_{et} and ζ_F depend on the direction of the emission transition dipole moment. The direction of the absorption transition dipole moment for the Q_y transition of P has been estimated by polarized absorption measurements on single crystals of *Rps. viridis* RCs²⁵ and by calculations.² It has been determined by fluorescence depolarization measurements that the absorption and emission transition dipole moments in *Rb. sphaeroides* RCs are nearly parallel.²⁶ If the emitting state is the same as the state formed upon excitation into the Q_y band of P, then ζ_F should be equal to ζ_A , given in (2) above.

(5) γ is the angle between $\Delta\mu_{et}$ and $-\Delta\mu_F$. Given the approximations in (1) and (2), it is the angle between $\mu(^1P)$ and

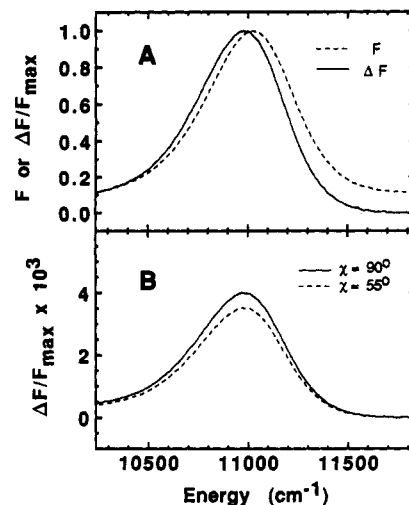


Figure 5. (A) Dashed line: fluorescence spectrum of Q-depleted *Rb. sphaeroides* RCs in PVA at 77 K. Solid line: change in the fluorescence spectrum for the same sample in an applied electric field with the experimental angle $\chi = 90^\circ$. The ΔF spectrum has been scaled to the same amplitude as the fluorescence spectrum to facilitate comparison of their shapes and positions. (B) ΔF spectrum for an applied electric field of 1×10^5 V/cm with (solid line) $\chi = 90^\circ$ and (dashed line) $\chi = 55^\circ$. The experimental ΔF spectra shown here were obtained at an applied electric field of 8.9×10^5 V/cm and have been scaled to the value of $\Delta F/F_{max}$ observed at an applied field of 1×10^5 V/cm to facilitate comparison with the calculated spectra in Figure 4 (no significant line-shape changes have been observed between 10^5 and 10^6 V/cm). The line shape of the ΔF spectrum and the dependence of $\Delta F/F_{max}$ on χ are the same for Q_A -depleted and Q_A -containing RCs.

either $\mu(P^{*+}H_L^{-})$ or $\mu(P^{*+}B_L^{-})$, i.e., the angle between the permanent electric dipole moments of the initial and final states of the electron-transfer reaction; its value is to be determined.

(6) P_1 , P_2 , and P_3 are the coefficients for the linear, quadratic, and cubic terms in the equation for the dependence of Φ_F on the electric-field perturbation (eq 3). The coefficients P_1 , P_2 , and P_3 determine the shape of the Φ_F versus electric-field curve. If the primary effect of the electric field on the electron-transfer reaction is due to a change in the free energy difference between the electron-transfer initial and final states by an amount $-\Delta\mu_{et}\cdot F_{int}$, then the values of P_1 , P_2 , and P_3 can be interpreted as defining the rate versus free energy curve for this rapid, long-distance electron-transfer reaction, a matter of considerable fundamental interest (possible complications due to field effects on the electronic coupling are discussed in refs 2, 4, and 19). The coefficients have direct physical meaning with respect to the rate versus free energy curve since $\log k_{et}$ is simply a polynomial. A positive value of P_1 means that at zero field the reaction is in the normal region of the rate versus free energy curve (as opposed to the inverted region¹⁵), and a nonzero value of P_1 indicates that the rate at zero field is not the maximum but can be larger for a different value of ΔG_{et} . The sign of the odd-numbered terms P_i is not unique and therefore must be obtained from additional data or theoretical considerations. This problem exists even in an oriented sample if both aligned and opposite orientations are present. In discussing the sign of $\cos \gamma$ (see below), we refer to the sign of P_1 as representative of all of the odd-powered terms in the cumulant expansion. The magnitude of $\Delta F/F_{max}$ and the line shape of the ΔF spectrum are very sensitive to the values of P_1 , P_2 , and P_3 , and their values are to be determined.

Experimental Constraints. The experimental constraints for the case of the RC are listed below.

(1) The sign, magnitude, and field dependence of the relative change in the net fluorescence quantum yield, $\Delta F/F_{max}$, and its line shape (Figure 5): These are determined primarily by $|\Delta\mu_{et}|$ and the coefficients P_1 , P_2 , and P_3 for a given field. For an externally applied electric field of 10^6 V/cm, the relative change in the fluorescence yield in Q_A -containing *Rb. sphaeroides* RCs in PVA at 77 K is observed to be about 40%. Between 10^5 and 10^6 V/cm the magnitude of $\Delta F/F_{max}$ is found to increase with

(22) Deisenhofer, J.; Epp, O.; Miki, K.; Huber, R.; Michel, H. *J. Mol. Biol.* **1984**, *180*, 385-398.

(23) Deisenhofer, J.; Epp, O.; Miki, K.; Huber, R.; Michel, H. *Nature* **1985**, *318*, 618-624.

(24) Michel, H.; Epp, O.; Deisenhofer, J. *EMBO J.* **1986**, *5*, 2445-2451.

(25) Zinth, W.; Sander, M.; Dobler, J.; Kaiser, W. In *Springer Series in Chemical Physics on Antennas and Reaction Centers of Photosynthetic Bacteria*; Michel-Beyerle, M. E., Ed.; Springer, Berlin, 1985; Vol. 42, p 97.

(26) Ebrey, T. G.; Clayton, R. K. *Photochem. Photobiol.* **1969**, *10*, 109.

a very slightly subquadratic dependence on field strength,^{1,2} and the experimentally observed shape of the ΔF spectrum is nearly independent of field over this range.

(2) The magnitude and direction of the shift in the wavelength maximum of the ΔF spectrum relative to the fluorescence spectrum (Figure 5): The direction of the shift (for $\chi = 90^\circ$, where χ is the experimental angle between the direction of the applied electric field and the polarization direction of the polarizer through which the fluorescence is collected) is determined primarily by γ and the coefficients P_1 , P_2 , and P_3 . The observed ΔF spectrum is shifted to the red (lower energy) relative to the fluorescence spectrum by about 60 cm^{-1} for the experimental angle χ equal to 90° .⁵³

(3) The width and overall shape of the ΔF spectrum: The observed ΔF spectrum (Figure 5) has nearly the same width as the fluorescence spectrum and has no additional features or substantial asymmetry.

(4) The dependence of the following on the experimental angle χ between the direction of the applied electric field and the polarization direction of the polarizer through which the fluorescence is collected (the analyzing polarizer): the shift of the ΔF spectrum, the value of $\Delta F/F_{\text{max}}$, and the width and overall shape of the ΔF spectrum. The magnitude of the red shift is observed to be nearly independent of the experimental angle χ for values of χ between 90 and 55° , the width and overall shape of the ΔF spectrum are nearly independent of χ , and the magnitude of $\Delta F/F_{\text{max}}$ decreases by about 12% as χ is changed from 90 to 55° (see Figure 5B).

(5) The RC X-ray crystal structure²²⁻²⁴ and the results of transient absorption measurements,²⁷⁻³² absorption Stark effect measurements,^{8,9} polarized absorption on RC single crystals,²⁵ and fluorescence depolarization studies:²⁶ The X-ray structure coordinates are used to estimate the magnitude and directions of the dipoles of the relevant states.⁵² The transient absorption and stimulated emission measurements indicate that the emitting state lives for about 2 ps at 77 K and room temperature and that the state $\text{P}^+\text{H}_\text{L}^-$ is formed with approximately the same time constant.^{27-33,54} The absorption Stark effect experiment on the Q_y band of P indicates that $|\Delta\mu_\text{A}|$ is about 7 D/f at 77 K and that $\zeta_\text{A} = 38 \pm 2^\circ$.^{8,9} The polarized absorption measurements on RC single crystals have been used to determine the approximate direction of the Q_y transition dipole moment of P,²⁵ and the fluorescence depolarization studies indicate that the fluorescence transition dipole moment is in approximately the same direction.²⁶

Model Calculation for an Oriented Sample. It is easier to conceptualize the origin of the effects giving rise to altered emission line shapes in an oriented sample than in an isotropic sample. For the purpose of illustration we treat the case of an oriented sample with two equal populations, one with the local C_2 axis of the RC aligned with and the other with the axis opposing the applied electric field in Figure 3. This is directly relevant to the case of RCs aligned in Langmuir-Blodgett films or lipid bilayers; an isotropic sample is simply the appropriate orientational average of this result. Many of the parameters used to generate Figure 3 are relevant to the RC problem; however, the primary purpose of this figure is to provide a simple example of the physical origin of unusual ΔF spectra when field-dependent processes compete with fluorescence. The magnitude of the effect of the electric field on the competing process, given by eq 3, is highly dependent on the angle θ between the electron-transfer difference dipole $\Delta\mu_\text{et}$ and the applied field F_int (i.e., the projection of $\Delta\mu_\text{et}$ along the field). To obtain information on the parameters P_i , it is necessary to

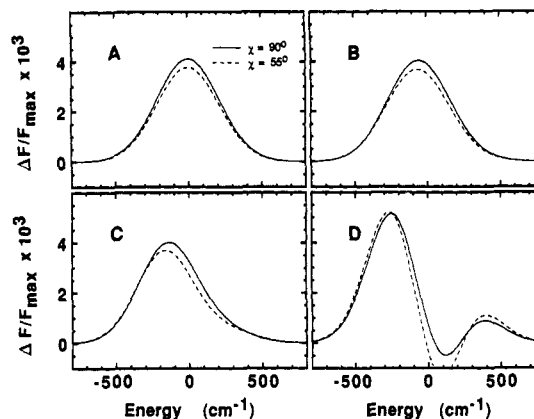


Figure 6. Calculated ΔF spectra demonstrating the effect of varying $|\Delta\mu_\text{F}|$, the dipole moment difference between the emitting state and the ground state, with $|\Delta\mu_\text{F}|$ equal to (A) 0 D, (B) 5 D, (C) 10 D, and (D) 20 D, for a field of $1 \times 10^5 \text{ V/cm}$ and $\chi = 90^\circ$ (solid lines) and $\chi = 55^\circ$ (dashed lines). Other parameters in the model were set as follows (see text): $|\Delta\mu_\text{et}| = 80 \text{ D}$, $\zeta_\text{F} = 38^\circ$, $\zeta_\text{et} = 65^\circ$, $\gamma = 153^\circ$, $P_1 = 0.67 \times 10^{-3}$, $P_2 = -0.4 \times 10^{-6}$, $P_3 = -0.23 \times 10^{-9}$, $F_\text{int} = 1 \times 10^5 \text{ V/cm}$.

compare data at many field values since each value gives one electric-field-modulated rate. The shape of the ΔF spectrum in this example is expected to be strongly dependent on field because each field value gives rise to a unique value of $\Phi_\text{F}(F_\text{int})$. By contrast, for an isotropic sample, the change in the emission line shape gives information on the orientation average of all values of the electric-field-dependent rate constant that are sampled in the presence of an electric field of a given magnitude.

The magnitude of the band shift in an oriented sample is a sensitive function of the projection of the difference dipole moment for fluorescence $\Delta\mu_\text{F}$ on a vector parallel to the field. In an oriented sample this projection is the same (but with opposite direction relative to the lab frame Z axis) for the molecules in each of the two populations and is defined by a fixed value of the azimuthal angle ϕ in the molecular frame. Compared to an isotropic sample, much larger effects are possible in an oriented sample, but they may not be observed if the projection of $\Delta\mu_\text{F}$ along the electric field vector is small. If there is no competing process (and no change in the polarizability tensor between the ground and excited state) the band shift for both opposed and aligned orientations will be equal but in opposite directions. In this case the emission line shape is calculated with all of the parameters P_i set to zero. The band shifts shown in Figure 3A are symmetric about the zero-field emission maximum. This situation gives rise to a second-derivative shaped ΔF spectrum as shown in Figure 3B.

If a competing process has only a linear term P_1 in its field dependence, the population for which the competing rate constant is increased will have less emission, while the opposite orientation, for which the rate constant is decreased in magnitude, will have enhanced emission. This situation gives rise to a shift in the emission line shape as shown in Figure 3C,D. The direction of the shift will be determined by the sign of P_1 as well as the angle γ between the vectors $\Delta\mu_\text{et}$ and $-\Delta\mu_\text{F}$. If P_1 is positive and the projections of $-\Delta\mu_\text{F}$ and $\Delta\mu_\text{et}$ are in the same direction ($\gamma < 90^\circ$), the population whose fluorescence has been shifted to higher energy than the zero-field maximum will have enhanced fluorescence giving rise to a blue shift in the ΔF spectrum. If the sign of P_1 is reversed or if $\gamma > 90^\circ$, a red shift in the ΔF spectrum will be observed. In Figure 3C,D a positive linear term has been included ($P_1 = 6.0 \times 10^{-4}$ with the interaction energy in units of cm^{-1}) with $\gamma < 90^\circ$, which enhances the fluorescence quantum yield of the population of emitters with the projection of $\Delta\mu_\text{et}$ opposed to the field, giving rise to a blue shift in the calculated ΔF spectrum.

Results and Discussion

In the following we impose the requirement that *all* the experimental constraints be met simultaneously. As stated in the previous section, we find that specific experimental results impose

(27) Woodbury, N. W.; Becker, M.; Middendorf, D.; Parson, W. W. *Biochemistry* **1985**, *124*, 7516-7521.

(28) Martin, J. L.; Breton, J.; Hoff, A. J.; Migus, A.; Antonetti, A. *Proc. Natl. Acad. Sci. U.S.A.* **1986**, *83*, 957-961.

(29) Breton, J.; Martin, J. L.; Migus, A.; Antonetti, A.; Orszag, A. *Proc. Natl. Acad. Sci. U.S.A.* **1986**, *83*, 5121-5125.

(30) Fleming, G. R.; Martin, J.-L.; Breton, J. *Nature* **1988**, *333*, 190.

(31) Kirmaier, C.; Holten, *FEBS Lett.* **1988**, *239*, 211-218.

(32) Breton, J.; Martin, J.-L.; Fleming, G. R.; Lambry, J. C. *Biochemistry* **1988**, *27*, 8276-8284.

(33) Holzapfel, W.; Finkle, U.; Kaiser, W.; Oesterheld, D.; Scheer, H.; Stilz, H. U.; Zinth, W. *Chem. Phys. Lett.* **1989**, *160*, 1-7.

rather narrow limits on some of the unknown parameters. Thus, the values of these parameters are overdetermined by the experimental data. Furthermore, the physical arrangement of the reactive chromophores in the RC imposes obvious limits on the distance- and angle-dependent parameters.

(1) *Magnitude of $\Delta\mu_F$* : The original purpose of the fluorescence electric field effect experiment on RCs¹ was to determine if $\Delta\mu_F$ is larger than $\Delta\mu_A$. The analysis in ref 1 assumed an isotropically weighted distribution of emitting molecules and indicated that $\Delta\mu_F$ is not larger than $\Delta\mu_A$ and may be much smaller. We now further investigate this question using the model that takes the effects of the field due to both $\Delta\mu_{et}$ and $\Delta\mu_F$ and the coupling between them into consideration. Figure 6 shows a series of model calculations of the ΔF spectrum for an isotropic sample using different values of $|\Delta\mu_F|$, with the other parameters fixed at values that lead to features that are qualitatively consistent with the data (primarily the red shift of the ΔF spectrum, the magnitude of $\Delta F/F_{max}$, and the small change in the ΔF spectrum as a function of χ , as further discussed below). It is evident that the ΔF spectrum can have a surprisingly wide range of line shapes, depending on the values of the various parameters. Many of the possible ΔF line shapes cannot be simply described by a sum of amplitude changes, shifts, and broadenings (zeroth, first, and second derivative shaped contributions, respectively). For parameters other than those used in Figure 6, much more extreme line shapes are possible: the shift of the ΔF spectrum can be in the opposite direction, the line width can be considerably greater, the dependence of the shape of the ΔF spectrum on χ can be very strong, and much greater asymmetry and additional spectral features are possible. These are not shown in the interest of brevity and because they are not observed experimentally in the RC. They may be important for the analysis of the results obtained on other electron-transfer systems, such as RC mutants or simple model systems.

The fact that the experimentally observed ΔF spectrum exhibits features that can be described primarily by an amplitude change and a small red shift of the fluorescence spectrum immediately places severe limits on the possible values of the parameters. In fact, the observed relatively small shift and the lack of a significant difference in width or asymmetry between the fluorescence and the ΔF spectrum, combined with the amplitude of $\Delta F/F_{max}$, leads to the conclusion that $|\Delta\mu_F|$ is less than 10 D and perhaps much less. Thus, the conclusion from the original paper¹ that $\Delta\mu_F$ is not much larger than $\Delta\mu_A$ is supported and better justified by the current more complete analysis.

Because the parameters that are considered interact in complex ways, parameter space was searched systematically to find agreement between the model calculations and the experimental data. A simulated annealing program was used to explore parameter space, constraining the ΔF spectrum to have the experimentally obtained shape, shift, amplitude, angle dependence, and field dependence. The values of P_1 , P_2 , P_3 , and γ were allowed to vary, while the other parameters were fixed at reasonable values. This procedure was done for different values of $|\Delta\mu_F|$ in order to determine the range of possible values of $|\Delta\mu_F|$. A particularly important constraint is the magnitude of the overall change in the fluorescence intensity (and its approximately quadratic field dependence). This is complicated by two issues. The first is the possibility of contaminating fluorescence from RCs which may emit in the 870–1000-nm region but have a degraded function. Because the RC fluorescence quantum yield is low, the presence of a small amount of damaged RCs (ones that do not efficiently perform electron transfer and thus might have a considerably higher and field-independent quantum yield) could cause the observed value of $\Delta F/F_{max}$ to be smaller than the value determined solely by the change in k_{et} . It is unlikely that this is a significant problem on the basis of recent direct measurements of the electric-field effect on the initial electron-transfer kinetics^{3,4} and by the fact that the magnitude of $\Delta F/F_{max}$ and the line shape of the ΔF spectrum observed by using many RC samples from different preparations and laboratories, including samples of *Rps. viridis* RCs [D. J. Lockhart and S. G. Boxer, unpublished results], are

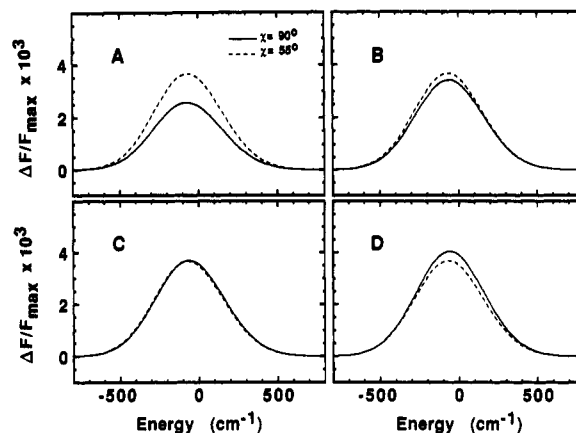


Figure 7. Calculated ΔF spectra for $F_{int} = 10^5$ V/cm, $\chi = 90^\circ$ (solid lines) and $\chi = 55^\circ$ (dashed lines). The ΔF spectra are calculated by using $|\Delta\mu_{et}| = 80$ D, $\zeta_F = 38^\circ$, $P_1 = 0.67 \times 10^{-3}$, $P_2 = -0.4 \times 10^{-6}$, $P_3 = -0.23 \times 10^{-9}$, $|\Delta\mu_F| = 5$ D, and $\gamma = 153^\circ$. (A) $\zeta_{et} = 25^\circ$: The amplitude of the ΔF spectrum at $\chi = 55^\circ$ is larger than that at $\chi = 90^\circ$, which is the opposite direction of the experimentally observed trend. (B) $\zeta_{et} = 48^\circ$: The ΔF spectrum at $\chi = 55^\circ$ is slightly larger than that at $\chi = 90^\circ$. (C) $\zeta_{et} = 55^\circ$: The ΔF spectra at $\chi = 55^\circ$ and $\chi = 90^\circ$ are almost identical. (D) $\zeta_{et} = 65^\circ$: The amplitude of the ΔF spectrum at $\chi = 55^\circ$ is smaller than that at $\chi = 90^\circ$ and the fwhm for $\chi = 90^\circ$ is 525 cm^{-1} .

similar. In addition, independent measurements in the laboratory of Professor Michel-Beyerle agree quantitatively with our results [M. E. Michel-Beyerle, personal communication]. The second complication is the uncertain value of the internal field correction factor, f . A value of f greater than 1 has the effect of reducing the upper limit for the value of $|\Delta\mu_F|$. The calculations were done initially assuming that $f = 1$ and that the observed value of $\Delta F/F_{max}$ is unaffected by contaminating fluorescence, i.e., that $\Delta F/F_{max}$ is indicative of the change in Φ_F due solely to a change in k_{et} .

If $|\Delta\mu_F|$ is fixed at a value of 10 D or larger, we are unable to find a set of parameters that result in a calculated fluorescence electric field effect that satisfies all of the experimental constraints. If $|\Delta\mu_F|$ is set at a value of 6 D, reasonable agreement can be obtained with the agreement becoming better if $|\Delta\mu_F|$ is between 3 and 5 D (see Figure 6). It is impossible, within this model, for the ΔF spectrum to be shifted if $|\Delta\mu_F|$ is zero (see Figure 6 and eq 4), but reasonable agreement can be obtained, if $|\Delta\mu_F|$ is between 1 and 3 D. On the basis of this analysis, the value of $|\Delta\mu_F|$ is conservatively estimated to be in the range between $1/f$ and $10/f$ D. Although we give this large range, the results provide the essential information that the emitting state is not significantly more dipolar than the absorbing state, ruling out a subpicosecond electronic decay process to one or more charge-transfer states prior to the transfer of an electron to H_L . Combined with the observation that the transition dipole moments for the Q_y absorption band of P and the RC fluorescence are nearly parallel,²⁶ the determination that $|\Delta\mu_F|$ is not significantly larger than $|\Delta\mu_A|$ indicates that it is likely that the emission from RCs comes from a state that is essentially the same as the state formed upon direct electronic excitation of P. This leads to the physically reasonable conclusion that $\Delta\mu_A \approx -\Delta\mu_F$.

(2) ζ_{et} : The angle ζ_{et} between $\Delta\mu_{et}$ and the emission transition dipole moment was determined to be $69 \pm 4^\circ$ from an analysis of the dependence of $\Delta F/F_{max}$ on the experimental angle χ .² This value of ζ_{et} was used to argue against a two-step hopping mechanism in which an electron is initially transferred to the nearby bacteriochlorophyll monomer, B_L , prior to the formation of the state $P^{+}H_L^{-}$.³ For the two-step hopping mechanism, ζ_{et} is expected to be about 49° .⁵² This earlier analysis reasonably ignored the effects due to $\Delta\mu_F$ discussed here based on the observation that the dominant effect of the field was on Φ_F (the fluorescence amplitude) through $\Delta\mu_{et}$. The more complete treatment described in this paper supports this earlier conclusion. Because the dominant effect of the field is on the amplitude of the fluorescence

band, the dependence of the value of $\Delta F/F_{\max}$ on χ is, in fact, found to depend primarily, but not exclusively, on ζ_{et} (see Figure 7). Figure 7B shows the ΔF spectra calculated by using $\zeta_{\text{et}} = 48^\circ$. For this angle the value of $\Delta F/F_{\max}$ is calculated to increase as χ is decreased from 90 to 55° , contrary to the experimental results (Figure 5B). If $|\Delta\mu_{\text{F}}|$ is 5 D and $\zeta_{\text{F}} = \zeta_{\text{A}} = 38^\circ$, then the observed angle dependence of $\Delta F/F_{\max}$ is found to be consistent with $\zeta_{\text{et}} \sim 65^\circ$ instead of 69° (Figure 7D). Thus, it is possible that some of the difference between the value of ζ_{et} predicted from the RC X-ray crystal structure for a direct electron-transfer reaction between P and H_L (58°)^{2,22} and the experimentally determined value obtained earlier may be accounted for by this more complete analysis. We were unable to find a set of parameters for which a value of $\zeta_{\text{et}} < 60^\circ$ could be used while obtaining a calculated result that was consistent with the experimental observations (primarily the dependence of $\Delta F/F_{\max}$ on χ as shown in Figure 7), supporting the earlier arguments against the two-step hopping mechanism.⁵⁴

(3) ζ_{F} : If the emitting state is identical with the state formed upon direct electronic excitation into the Q_y band of P, then not only is $|\Delta\mu_{\text{F}}|$ expected to be about equal to $|\Delta\mu_{\text{A}}|$, but also ζ_{F} is expected to equal ζ_{A} , determined experimentally to be $38 \pm 2^\circ$.^{8,9} The current analysis, however, is not particularly sensitive to ζ_{F} because the effects due to $\Delta\mu_{\text{F}}$ are relatively small compared to those due to $\Delta\mu_{\text{et}}$. All that can be said is that a value of ζ_{F} equal to ζ_{A} is not inconsistent with the observables, but at the present time the analysis cannot prove the equality.

(4) γ : γ is the angle between $\Delta\mu_{\text{et}}$ and $-\Delta\mu_{\text{F}}$, the angle between the permanent electric dipole moments of the initial and final states of the electron-transfer reaction (assuming that the permanent dipole moment of the ground state of P is small). Taking $\Delta\mu_{\text{et}}$ as pointing approximately from $\text{H}_L^{\bullet-}$ to $\text{P}^{\bullet+}$ ⁵⁴ (then $\Delta\mu_{\text{et}} \sim \mu(\text{P}^{\bullet+}\text{H}_L^{\bullet-})$), an estimate of γ allows the determination of the direction of $\Delta\mu_{\text{F}}$ relative to the direction of the initial electron movement in the RC. This is valuable additional information for which there is no direct experimental evidence to date. From the angle dependence of the absorption Stark effect on the Q_y band of P, it was determined that $\zeta_{\text{A}} = 38 \pm 2^\circ$.^{8,9} Since the Q_y transition dipole moment of P is approximately perpendicular to the RC C_2 symmetry axis, the fact that ζ_{A} equals 38° and not 90° indicates that the electron density in ^1P is greater on either the L or M side.¹² Unfortunately, the measurement of ζ_{A} cannot determine which of the two sides is favored because the transition dipole is nearly perpendicular to the RC C_2 symmetry axis and transition dipoles are lines and not vectors, i.e., the absorption Stark effect measurement is sensitive to $\cos^2 \zeta_{\text{A}}$, so that the absolute direction of $\Delta\mu_{\text{A}}$ is not determined. The analysis presented here does not suffer from this shortcoming because γ is the angle between two vectors, with one of them, $\Delta\mu_{\text{et}}$, constrained to point along the L side in the direction from either H_L or B_L to P, and the observable is sensitive to the cosine of γ and not the cosine squared. From the model calculations the observable that is found to be determined primarily by γ is the direction of the wavelength shift in the ΔF spectrum relative to the fluorescence spectrum. For $|\Delta\mu_{\text{F}}| \sim 5$ D the calculated dependence of the red shift on the experimental angle χ becomes weaker as γ approaches 180° . For $\zeta_{\text{F}} = 38^\circ$ and $\zeta_{\text{et}} = 65^\circ$ the maximum possible value of γ is 153° (for geometric reasons). For appropriate choices of P_1 , P_2 , and P_3 and using $|\Delta\mu_{\text{F}}| = 5$ D and $\gamma = 153^\circ$, it is seen that the calculated red shift is about 55 cm^{-1} for $\chi = 90^\circ$ increasing slightly to about 68 cm^{-1} for $\chi = 55^\circ$ with almost no change in line shape (see Figure 6B), consistent with the experimental results⁵² (note that the calculated magnitude of $\Delta F/F_{\max}$, the change in $\Delta F/F_{\max}$ as a function of χ , and the field dependence of $\Delta F/F_{\max}$ using this set of parameters are also consistent with the experimental results).

As shown above, it is reasonable to conclude that $-\Delta\mu_{\text{F}} \approx \Delta\mu_{\text{A}}$ and that the state ^1P is moderately dipolar. It has been postulated that this state is dipolar due to mixing with intradimer charge-transfer states,^{12,49-51} denoted $\text{P}^{\bullet+}\text{P}^{\bullet-}$. Approximating the electronic distributions of the anion and cation radicals involved in this problem as point charges located at the center of their respective

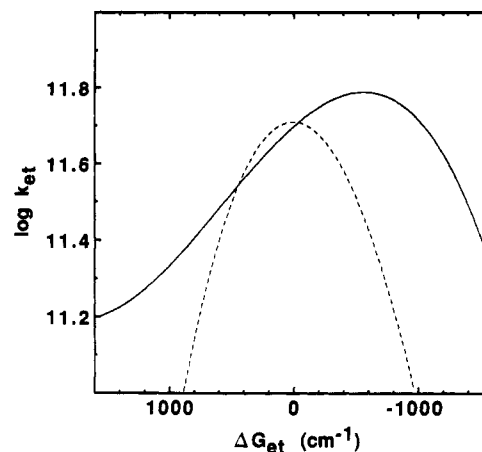


Figure 8. (—) Plot of the $\log k_{\text{et}}$ versus ΔG_{et} (the change in the value of ΔG_{et} due to the presence of the applied electric field) curve. This curve is obtained by using the parameters $P_1 = 0.67 \times 10^{-3}$, $P_2 = -0.4 \times 10^{-6}$ and $P_3 = -0.23 \times 10^{-9}$, which give rise to a calculated ΔF spectrum that is consistent with the experimental results, assuming that the primary effect of the field is due to a change in ΔG_{et} by an amount $-\Delta\mu_{\text{et}} \cdot \mathbf{F}$, with $|\Delta\mu_{\text{et}}| = 80$ D, $f = 1$, and $|\Delta\mu_{\text{F}}| = 5$ D. (---) Dependence of k_{et} on ΔG_{et} using the single-mode, quantum mechanical treatment of Jortner et al. with $h\nu = 100 \text{ cm}^{-1}$ and $\lambda = -\Delta G_{\text{et}}(\text{F}_{\text{int}}=0) = 2000 \text{ cm}^{-1}$ at 77 K, and the electronic coupling $V = 25.7 \text{ cm}^{-1}$ (V field independent). A similar dependence is obtained by using the semiclassical Marcus theory expression for k_{et} with $\lambda = -\Delta G_{\text{et}}(\text{F}_{\text{int}}=0) = 2000 \text{ cm}^{-1}$ at 77 K.

macrocycles, the directions of the various state dipoles can be calculated by using the *Rps. viridis* X-ray structure coordinates.^{22-24,52} If $-\Delta\mu_{\text{F}}$ is in the direction of $\mu(\text{P}_M^{\bullet+}\text{P}_L^{\bullet-})$ and $\Delta\mu_{\text{et}} \sim \mu(\text{P}^{\bullet+}\text{H}_L^{\bullet-})$, then γ is expected to be about 68° . If $-\Delta\mu_{\text{F}}$ is in the direction of $\mu(\text{P}_L^{\bullet+}\text{P}_M^{\bullet-})$, then γ is expected to be about 112° . Since a value of $\gamma > 90^\circ$ is required to meet the constraint imposed by the red shift in the ΔF spectrum, this suggests that if $\Delta\mu_{\text{F}}$ is determined primarily by mixing with intradimer charge-transfer states, the state that is likely to be important is $\text{P}_L^{\bullet+}\text{P}_M^{\bullet-}$. This is consistent with the hypothesis that additional electron density on P_M favors electron transfer to H_L because of the arrangement of the chromophores and slight structural asymmetry in the RC.³⁴⁻³⁷ These conclusions are dependent on the assumptions that $P_1 > 0$ (i.e., that the electron-transfer reaction is in the normal region at zero field) and that the ground state of P is relatively nonpolar.

(5) *Rate versus free energy curve*: We have argued that $\Phi_{\text{F}} \propto 1/k_{\text{et}}$ and that both k_{et} and Φ_{F} are altered due to a change in the energy difference between the initial and final states of the electron-transfer reaction according to eq 3. If the primary effect of the electric field is due to a change in ΔG_{et} by an amount $-\Delta\mu_{\text{et}} \cdot \mathbf{F}$, then the coefficients P_1 , P_2 , and P_3 define the rate versus free energy curve for this rapid, long-distance electron-transfer reaction. Possible effects of the field on the electronic coupling between the initial and final states are discussed in refs 4, 12, 19, and 38; it is shown that these effects are likely considerably smaller

(34) Plato, M.; Möbius, K.; Michel-Beyerle, M. E.; Bixon, M.; Jortner, J. *J. Am. Chem. Soc.* **1988**, *110*, 7279-7285.

(35) Michel-Beyerle, M. E.; Plato, M.; Deisenhofer, J.; Michel, H.; Bixon, M.; Jortner, J. *Biochem. Biophys. Acta* **1988**, *932*, 52-70.

(36) Allen, J. P.; Feher, G.; Yeates, T. O.; Komiya, H.; Rees, D. C. In *The Photosynthetic Bacterial Reaction Center—Structure and Dynamics*; Breton, J., Vermeglio, A., Eds.; Plenum: New York, 1988; pp 5-11.

(37) Scherer, P. O. J.; Fischer, S. F. *J. Phys. Chem.* **1989**, *93*, 1633-1637.

(38) Bixon, M.; Jortner, J. *J. Phys. Chem.* **1988**, *92*, 7148-7156.

(39) Jortner, J. *J. Am. Chem. Soc.* **1980**, *102*, 6676-6686.

(40) Plato, M.; Lendzian, F.; Lubitz, W.; Tränkle, E.; Möbius, K. In *The Photosynthetic Bacterial Reaction Center—Structure and Dynamics*; Breton, J., Vermeglio, A., Eds.; Plenum: New York, 1988; pp 379-388.

(41) Allen, J. P.; Feher, G.; Yeates, T. O.; Komiya, H.; Rees, D. C. *Proc. Natl. Acad. Sci. U.S.A.* **1987**, *84*, 5730-5734.

(42) Allen, J. P.; Feher, G.; Yeates, T. O.; Komiya, H.; Rees, D. C. *Proc. Natl. Acad. Sci. U.S.A.* **1987**, *84*, 6162-6166.

(43) Chang, C. H.; Tiede, D.; Tang, J.; Smith, U.; Norris, J. *FEBS Lett.* **1986**, *205*, 82-86.

than those due to the change in ΔG_{et} . As discussed in the previous section, we use $P_1 > 0$. The value of P_1 determines the vertical and horizontal difference between the zero-field position and the maximum of the rate versus free energy curve (how nearly optimally exergonic the reaction is at zero field, determined by the difference between λ and ΔG_{et} in a semiclassical Marcus theory treatment¹⁵). We have assumed that $\Delta\mu_{et}$ is determined primarily by $\mu(P^{+}H_L^{-})$ and therefore set $|\Delta\mu_{et}|$ equal to 80 D.⁵³ For $f = 1$, $|\Delta\mu_F| = 5$ D, and $|\Delta\mu_{et}| = 80$ D, the values of P_1 , P_2 , and P_3 that give rise to a ΔF spectrum consistent with all the experimental

(44) Van Kampen, N. G. *Stochastic Processes in Physics and Chemistry*; Elsevier Science: New York, 1981; pp 6–8.

(45) Stoneham, A. M. *Rev. Mod. Phys.* **1969**, *41*, 82–108.

(46) Lax, M. *J. Chem. Phys.* **1952**, *20*, 1752–1769.

(47) Liptay, W. *Z. Naturforschung* **1965**, *20a*, 272–289.

(48) Lin, S. H. *J. Chem. Phys.* **1975**, *62*, 4500–4524.

(49) Won, Y.; Friesner, R. A. *J. Phys. Chem.* **1988**, *92*, 2214–2219.

(50) Warshel, A.; Creighton, S.; Parson, W. W. *J. Phys. Chem.* **1988**, *92*, 2696–2701.

(51) Scherer, P. O. J.; Fischer, S. F. *Chem. Phys. Lett.* **1986**, *131*, 153–159.

(52) For the purposes of calculating the magnitudes and directions of the permanent electric dipole moments of the charge-separated states, we have assumed that the charge distributions in the anion and cation radicals can be approximated by point charges located at the geometric centers of the macrocycles (the geometric center of dimeric P is defined as the point midway between the centers of the overlapping rings I of the monomeric bacteriochlorophylls that comprise P). Note that it is the electron density in the ions when both are present on the picosecond time scale that is relevant. It is conceivable that the electron densities in P^{+} are very different on a short time scale from those at longer time or even that proton motion compensates for one or the other charge. On the basis of the results of calculations of the electron density of P^{+} , it has been suggested that the center of charge in P^{+} is not located at the geometric center but instead is displaced in the direction of the L-side half of the dimer.⁴⁰ Considered alone, this changes the estimates of $\zeta_{et}(P^{+}B_L^{-})$ and $\zeta_{et}(P^{+}H_L^{-})$. However, these same calculations also predict that the permanent electric dipole moment of the state 1P points approximately from P_M to P_L (ref 40, and M. Plato, personal communication) (where P_M and P_L denote the M and L side halves of dimeric P). ζ_{et} is the angle between the difference dipole, $\Delta\mu_{et} = \mu(P^{+}I^{-}) - \mu(^1P)$, where I denotes the initial electron acceptor, and the fluorescence transition dipole moment. Because $\Delta\mu_{et}$ is a difference dipole, the effects of having the center of charge of P^{+} displaced toward P_L and having $\mu(^1P)$ pointing from P_M to P_L tend to cancel when the difference is taken. In other words, if 1P and P^{+} deviate from being nonpolar and electronically symmetric, respectively, and if the deviations are in the same direction, then the direction of $\Delta\mu_{et}$ is largely unaffected. Thus, the difference dipole that is relevant for the electric-field effect on the initial electron-transfer reaction, $\Delta\mu_{et}$, is still expected to point approximately along the line between the geometric centers of the chromophores. No such cancellation occurs if the center of charge in B_L^{-} or H_L^{-} is not located at the geometric center of the macrocycles. These estimates for ζ_{et} can be readily modified in light of new information obtained on the charge distributions in these ions in the RC on the appropriate time scale.

(53) There is a potential problem in quantifying the small red shift of the ΔF spectrum relative to the fluorescence spectrum due to the presence of a small amount of fluorescence to the blue of the band being analyzed. This fluorescence (probably from extraneous bacteriochlorophyll) overlaps somewhat with the emission from 1P , but it is not significantly affected by the field. This could cause the ΔF spectrum to appear to be red shifted relative to the observed fluorescence spectrum because overlap on the blue side tends to shift the position of the observed fluorescence maximum to the blue, but it will not affect the ΔF spectrum. On the basis of our observations of the shifts in the ΔF spectra for different samples (different RC preparations and amounts of blue fluorescence) and on simulations of this effect, we estimate that it contributes less than 20 cm^{-1} to the observed red shift of the ΔF spectrum. All else being equal, if the true red shift of the ΔF spectrum is smaller than 60 cm^{-1} , then the upper limits for $|\Delta\mu_F|$ and P_1 are decreased slightly.

(54) On the basis of room-temperature, subpicosecond transient absorption measurements, Zinth and co-workers have recently concluded that the state $P^{+}B_L^{-}$ is formed as a discrete intermediate prior to the formation of $P^{+}H_L^{-}$.³³ In this case, the initial electron acceptor is B_L^{-} and, in the absence of a subpicosecond decay of the state 1P , $\Delta\mu_{et} = \mu(P^{+}B_L^{-}) - \mu(^1P) \approx \mu(P^{+}B_L^{-})$. From the x-ray structure of *Rps. viridis*,^{22–24} $|\mu(P^{+}B_L^{-})|$ is estimated to be about 50 D. If $|\Delta\mu_{et}|$ is 50 D rather than 80 D, then all else being equal, the values of P_1 and P_2 must be increased by factors of 1.6 (80/50 = 1.6) and 1.6², respectively, in order to obtain the same calculated ΔF spectrum. The calculations in this paper were performed using $f = 1.0$, but it is possible that f is as large as 2. It is important to realize that the results obtained by using $|\Delta\mu_{et}| = 80$ D and $f = 1.0$ are equivalent to those obtained with $|\Delta\mu_{et}| = 50$ D and $f = 1.6$. This is one of the reasons that the magnitude of the field effects has not been used by us to establish the identity of the initial electron acceptor. The assignment of H_L^{-} as the likely initial electron acceptor is based primarily on the determination of the angle ζ_{et} , as described in the text and in ref 2. An analysis of the consequences of the identity of the initial electron acceptor in the context of the reaction energetics is discussed in detail elsewhere.^{4,12,38}

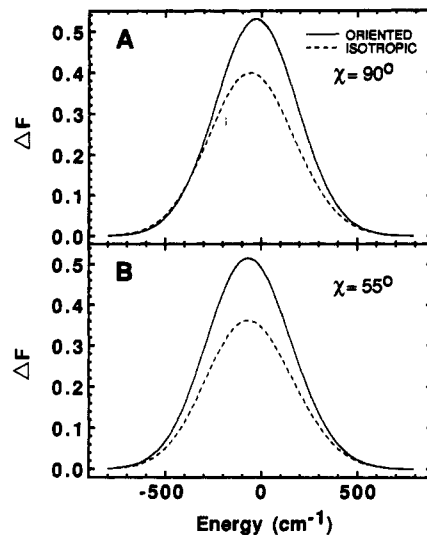


Figure 9. Calculated ΔF spectra for an oriented sample (—) and an isotropic sample (---) by using the parameters that best fit the data obtained on an isotropic sample: $|\Delta\mu_{et}| = 80$ D, $\zeta_{et} = 38^\circ$, $\zeta_{et} = 65^\circ$, $\gamma = 153^\circ$, $P_1 = 0.67 \times 10^{-3}$, $P_2 = -0.4 \times 10^{-6}$, $P_3 = -0.23 \times 10^{-9}$, $F_{int} = 1 \times 10^6$ V/cm. (A) $\chi = 90^\circ$; (B) $\chi = 55^\circ$.

data are $P_1 \sim 0.67 \times 10^{-3}$, $P_2 \sim -0.4 \times 10^{-6}$, and $P_3 \sim -0.23 \times 10^{-9}$ with the interaction energy of the dipole with the field in units of wavenumbers. The k_{et} versus $\Delta\Delta G_{et}$ (the change in the value of ΔG_{et} due to the field) curve that results by using these parameters is shown in Figure 8.

As discussed earlier and in refs 3 and 4, it is possible that the true value of $\Delta F/F_{max}$ determined by the change in k_{et} is larger by about a factor of 2. In this case, values of $P_1 \sim 1.2 \times 10^{-3}$, $P_2 \sim -0.57 \times 10^{-6}$, and $P_3 \sim -0.41 \times 10^{-9}$ would be consistent with the data. Given these considerations, we estimate conservatively that $0.6 \times 10^{-3} \leq P_1 \leq 1.2 \times 10^{-3}$, $-5.7 \times 10^{-7} \leq P_2 \leq -4.0 \times 10^{-7}$, and $-4.1 \times 10^{-10} \leq P_3 \leq -2.3 \times 10^{-10}$, noting that because the effects of the parameters are coupled, P_1 , P_2 , P_3 , and $|\Delta\mu_F|$ cannot be independently varied within the stated ranges.

The resulting rate versus free energy curve in Figure 8 is considerably flatter than that predicted from a semiclassical Marcus theory expression¹⁵ assuming $\lambda \sim -\Delta G_{et} = 2000$ cm^{-1} , or the quantum mechanical single-mode treatment of Jortner et al.^{36,37} (mode frequency $h\nu \sim 100$ cm^{-1} , and $\lambda = 2000$ cm^{-1} at 77 K). The latter is shown in Figure 8 for comparison. The values of P_1 , P_2 , and P_3 that are consistent with the data are dependent on f . All else being equal, if $f > 1$, the rate versus free energy curve that is consistent with the data will be even flatter. We note that the difference between the curves predicted by using the simplified versions of conventional electron-transfer treatments and the empirically obtained curve in Figure 8 is not just a matter of different magnitudes of P_1 , P_2 , and P_3 . These treatments predict a dependence of k_{et} on ΔG_{et} (through the nuclear or Franck-Condon weighted density of states term) that is approximately Gaussian, leading to a field dependence of $\Delta F/F_{max}$ significantly greater than quadratic over the range of fields used. Thus, with these treatments the predicted field dependence of $\Delta F/F_{max}$ is inconsistent with the experimental results (see ref 4 for details). The apparent inability of the quantum mechanical single-mode model to account for the observed value of $\Delta F/F_{max}$ and its field dependence suggests that a less simple analysis including a physically realistic distribution of low- and high-frequency modes may be required to adequately explain the electron-transfer reactions in the RC (a similar conclusion has been reached from an analysis of the electric-field effect on the slow $P^{+}Q_A^{-} \rightarrow PQ_A$ recombination reaction in *Rb. sphaeroides* RCs³⁸). The curve shown in Figure 8 is derived from the detailed analysis of the experimental dependence of the fluorescence on an electric field which provides a good test of any treatment of the initial electron transfer reaction in photosynthetic RCs.

(6) *Predictions for an oriented sample:* Using the parameters that are consistent with the data and information on the structure

of the RC obtained from the crystal structure, one can predict the ΔF spectrum for an oriented sample with equal populations aligned with and opposing the field direction. If one assumes that the RC is aligned so that the local C_2 symmetry axis of the RC is parallel to the applied electric field (a realistic case), then the angle between $\Delta\mu_{\text{el}}$ and \mathbf{F}_{int} is 48° (assuming $\Delta\mu_{\text{el}} = \mu(\text{P}^+\text{H}_L^-)$).⁵² The direction of $\Delta\mu_{\text{F}}$ is not uniquely specified by the angle γ . We have used information from polarized single-crystal spectroscopy²⁵ to define the direction of the Q_y transition moment of P. With this direction specified, the angle $\zeta_A = 38^\circ$ from the absorption Stark effect, and other parameters the same as in the case of an isotropic sample, the angle between $-\Delta\mu_{\text{F}}$ and \mathbf{F}_{int} is 47° . As shown in Figure 9, the effect of a field of 10^6 V/cm on the fluorescence is only slightly larger in this type of oriented sample than the orientationally averaged effect in an isotropic sample.⁴ This surprising result occurs because the projection of the dipoles in the RC along the field direction in a sample in which the local C_2 symmetry axis of the RC is aligned with the applied field is small (see Figure 4). The major difference between the result found for an isotropic sample (Figure 5) and that predicted for an oriented sample is that the band shift in an oriented sample is predicted to be slightly more strongly dependent on the angle χ . The maximum of the ΔF spectrum for an oriented sample is predicted to be only 20% larger than that for an isotropic sample and the spectrum has very nearly the same shape. One consequence of this result is that the effect of an electric field on the kinetics of the initial charge-separation step in an oriented sample is predicted to have approximately the same magnitude as that found by Lockhart et al. in an isotropic sample.⁴ The effect of an electric field on the fluorescence in an oriented sample is strongly dependent on the relative orientation of $\Delta\mu_{\text{F}}$ and \mathbf{F}_{int} as well as the magnitude of $\Delta\mu_{\text{F}}$. Since the observables are more sensitive to these parameter values for an oriented than an isotropic sample, the results of an experiment on an oriented sample will help to more accurately determine the values of the parameters

discussed here.

Summary of Results and Conclusions

The fluorescence from bacterial photosynthetic RCs has been found to be affected by an electric field. A model is presented that is a direct consequence of the usual scheme describing the initial events in the RC (Figure 2), and it is shown that the line shape and amplitude of the fluorescence change contain a wealth of information about the initial and final states of the picosecond long-distance electron-transfer reaction. Specifically, within reasonable assumptions, it is found that the constraints imposed by the experimental observation of the ΔF spectrum and its dependence on experimental conditions, combined with numerous other experimental observations, can be satisfied if (1) $-\Delta\mu_{\text{F}} \simeq \Delta\mu_{\text{A}}$, (2) $\zeta_{\text{el}} \simeq 65^\circ$, (3) $|\Delta\mu_{\text{el}}| \simeq 80$ D,⁵² (4) $\gamma \simeq 153^\circ$, (5) $0.6 \times 10^{-3} \leq P_1 \leq 1.2 \times 10^{-3}$, $-5.7 \times 10^{-7} \leq P_2 \leq -4.0 \times 10^{-7}$, and $-4.1 \times 10^{-10} \leq P_3 \leq -2.3 \times 10^{-10}$.

The values of these parameters are consistent with the following conclusions: (1) the emitting state in RCs is essentially the same as the state formed upon electronic excitation into the Q_y band of the special pair, i.e., the initially formed excited state of P does not decay on a subpicosecond time scale to a much more dipolar charge-transfer state and is most likely the initial state of the subsequent picosecond electron-transfer reaction; (2) the initial electron acceptor is likely H_L and not the nearby bacteriochlorophyll monomer, B_L ; (3) the intradimer charge-transfer state most likely to be important in determining the nature of 'P' is that with additional electron density on P_M and not P_L ; (4) the rate versus free energy curve for the initial electron-transfer reaction is similar to that shown in Figure 8, considerably flatter than that predicted for this reaction from the simplified versions of electron-transfer treatments commonly in use. The shape of the rate vs free energy curve is consistent with a substantial contribution from high-frequency modes to the reorganization energy for the initial charge-separation reaction.

Molecular Orbital Investigation of Coal Fragments and Model Compounds

Harriet F. Ades,^{*,†,§} Audrey L. Companion,[†] and K. R. Subbaswamy[‡]

Departments of Chemistry and of Physics and Astronomy and Center for Computational Sciences, University of Kentucky, Lexington, Kentucky 40506-0055 (Received: June 13, 1990; In Final Form: October 8, 1990)

Anderson's modified version of the extended Hückel molecular orbital method [Anderson, A. B. *J. Chem. Phys.* **1974**, *60*, 2477] has been used to study the bond cleavage in molecular fragments of interest in coal liquefaction. Results obtained are in qualitative agreement with experiments. The calculations are used to elucidate the action of a novel catalyst in the thermolysis of a model compound of recent interest.

1. Introduction

Most of our knowledge of the molecular structure of coal¹ comes from analytical chemical techniques and through studies involving model compounds. Other methods, such as solvent swelling studies,² give information about the degree of cross-linking between clusters in coal and the average molecular weight of the clusters. Through years of research, fairly detailed molecular models of at least one of the coal macerals, namely vitrinite, have been proposed. Although a single structural model for vitrinite cannot be presented, it is widely accepted that a model proposed by Shinn³ is consistent with most of the features obtained from chemical analyses for both coal and the products from liquefaction schemes

but does not necessarily exhibit the correct cross-linking patterns. A knowledge of the structure of coal is needed in the optimal design of catalysts and reaction conditions for coal liquefaction.

The Shinn model may be used as a prototype for coal on which to perform quantum chemical calculations and simulations in order to study the effect of structural constraints on reaction pathways and on reaction kinetics in coal liquefaction processes. Electronic structure calculations allow one to compare different geometric conformations and bond-breaking energies for molecules under a variety of conditions. For example, calculations may be used to explain how the addition of a catalyst affects bond-breaking selectivity and activation energies. Molecular modeling programs,

*To whom correspondence should be addressed.

[†] Department of Chemistry.

[‡] Department of Physics and Astronomy.

[§] Center for Computational Sciences.

(1) Davidson, R. M. *Molecular Structure of Coal*; ICTIS/TR 08; IEA Coal Research: London, 1980; 86 pp.

(2) Larsen, J. W.; Green, T. K.; Kovac, J. J. *Org. Chem.* **1985**, *50*, 4729.

(3) Shinn, J. *Proc. Int. Conf. Coal Sci.* **1985**, 738-741.